

OLD NEUTRON STARS AS PROBES OF ISOSPIN-VIOLATING DARK MATTER

HAO ZHENG¹, KAI-JIA SUN¹, AND LIE-WEN CHEN^{*1,2}¹ Department of Physics and Astronomy and Shanghai Key Laboratory for Particle Physics and Cosmology, Shanghai Jiao Tong University, Shanghai 200240, China and² Center of Theoretical Nuclear Physics, National Laboratory of Heavy Ion Accelerator, Lanzhou 730000, China*Draft version March 2, 2022*

Abstract

Isospin-violating dark matter (IVDM), which couples differently with protons and neutrons, provides a promising mechanism to ameliorate the tension among recent direct detection experiments. Assuming DM is non-interacting bosonic asymmetric IVDM, we investigate how the existence of old neutron stars limits the DM-proton scattering cross-section σ_p , especially the effects of the isospin violating DM-nucleon interactions and the symmetry energy in the equation of state of isospin asymmetric nuclear matter. Our calculations are completely based on general relativity and especially the structure of neutron stars is obtained by solving the Tolman-Oppenheimer-Volkoff equations with nuclear matter equation of state constrained by terrestrial experiments. We find that, by considering the more realistic neutron star model rather than a simple uniform neutron sphere as usual, the σ_p bounds from old neutron stars can be varied by more than an order of magnitude depending on the specific values of the DM neutron-to-proton coupling ratio f_n/f_p , and they can be further varied by more than a factor of two depending on the density dependence of the symmetry energy. In particular, we demonstrate that the observed nearby isolated old neutron star PSR B1257+12 can set a very strong limit on σ_p for low-mass DM particles (≤ 20 GeV) that reaches a sensitivity beyond the current best limits from direct detection experiments and disfavors the DM interpretation of previously-reported positive experimental results, including the IVDM.

Subject headings: dark matter - stars: neutron - dense matter - equation of state - astroparticle physics

1. INTRODUCTION

The quest for dark matter (DM) is one of the most intriguing aspects of current research frontiers of particle physics, astrophysics and cosmology. Cosmological observations have provided compelling evidence for the existence of DM. The most recent cosmological results based on *Planck* measurements of the cosmic microwave background (CMB) temperature and lensing-potential power spectra indicate that DM comprises about 27% of the energy density of the Universe which also contains about 5% baryon matter and about 68% dark energy (Ade et al. 2013). On the other hand, the DM nature and its interactions with the Standard Model particles remain unknown.

Many theories beyond the Standard Model of particle physics predict natural candidates for DM. Among them, motivated by the fact that the DM and baryon densities in the Universe are of the same order of magnitude, asymmetric dark matter (ADM) (Zurek 2014; Petraki & Volkas 2013) has been proposed as one of the most promising classes of candidates for DM. Having inherited a similar matter-antimatter asymmetry as baryons, the models of ADM mainly focus on the DM mass region around a few GeV. In this mass region, these models are favored by an excess of events over the expected background observed in some underground DM direct detection experiments such as CoGeNT (Aalseth et al. 2011), DAMA (Savage et al. 2009) and CRESSTII (Angloher et al. 2012) as well as the recent results presented by the CDMS-II(Si) collaboration (Agnese et al. 2013; Agnese & Ahmed et al.

2013). However, these observational evidences are in strong tension with the constraints set by some other experimental groups like XENON100 (Aprile et al. 2011, 2012), LUX (Akerib et al. 2014) and SuperCDMS(Ge) (Agnese et al. 2014).

Isospin-Violating Dark Matter (IVDM) provides a possible mechanism to reconcile the tension among different experiments (Kurylov & Kamionkowski 2004; Giuliani 2005; Chang et al. 2010; Feng et al. 2011, 2013; Feng & Kumar et al. 2013; Nagao & Naka 2013; Cirigliano et al. 2013; Zheng et al. 2014). Within the IVDM framework, DM is assumed to couple differently with protons and neutrons, and this assumption of the isospin violation has been supported by a number of theoretical works (Frandsen et al. 2011; Cline & Frey 2011; Nobile et al. 2012; He et al. 2012; Gao et al. 2013; Okada & Seto 2013) based on the particle physics point of view. Especially, IVDM can also be asymmetric in the model proposed by Okada and Seto in Ref. (Okada & Seto 2013).

Besides the underground DM direct detection experiments in terrestrial laboratory, the existence of old neutron stars in our Galaxy can also provide constraints on the scattering cross-sections between DM and nucleons. This subject was firstly studied by Goldman and Nussinov (Goldman & Nussinov 1989), and then a lot of works have been done during the last few years (Bertone & Fairbairn 2008; Lavallaz & Fairbairn 2010; Kouvaris & Tinyakov 2011; Kouvaris 2012, 2013; McDermott et al. 2012; Bramante et al. 2013, 2014; Jamison 2013; Bell et al. 2013; Guver et al. 2014). Especially for ADM, due to the asymmetry between particles and anti-particles in the DM sector, DM annihilation

* Corresponding author (email: lwchen@sjtu.edu.cn)

is not significant in this case. Therefore, DM can continually accumulate in the neutron star without depleting. After being thermalized through continually scattering with the neutron star matter, these DM particles will gather within a small thermal radius at the central region of the neutron star, then become self-gravitating and eventually collapse into black holes which could destroy the host neutron star.

For non-interacting fermionic DM, due to the Fermi degeneracy pressure, the required number for the self-gravitating DM to collapse into black holes (i.e., the Chandrasekhar limit) is about $(M_{\text{pl}}/m_\chi)^3$ (Colpi et al. 1986), where M_{pl} is the Planck mass and m_χ is the DM mass. Except for DM with a huge m_χ , this number is far beyond the amount of DM particles that could be captured by a neutron star within a few billion years inside a DM halo with density similar to that around the earth. On the other hand, for non-interacting bosonic DM the degeneracy pressure does not exist, and the relevant Chandrasekhar limit for collapsing becomes much smaller, i.e., about $(M_{\text{pl}}/m_\chi)^2$ (Colpi et al. 1986). This DM amount can be easily accumulated within the living age of a typical old neutron star if the DM-nucleon scattering cross-section is not too small. Furthermore, for the bosonic DM, the possible existence of the Bose-Einstein condensate (BEC) inside the neutron star could further facilitate the onset of self-gravitation, leading to an enhancement effect on the gravitational collapse. Once the mini black hole is formed inside the neutron star, it could subsequently lead to the ultimate destruction of the neutron star if it consumes the neutron star matter faster than the Hawking evaporation. However, old nearby neutron stars have been well observed, and this thus could result in a very severe constraint on the scattering cross-sections of the non-interacting bosonic ADM with nucleons. The above arguments are based on the assumption that the DM particles have no self-interactions (except for gravity). It should be mentioned that for fermionic DM, the required DM particle number for gravitational collapse can be strongly reduced if an attractive Yukawa force can appear among DM particles (Kouvaris 2012; Bramante et al. 2014). In addition, the repulsive self-interactions as well as the effect of DM-nucleon coannihilations can also prevent the black hole formation for bosonic DM (Bramante et al. 2013; Bell et al. 2013).

In previous studies, the neutron stars have been generally assumed to be consisted of pure neutrons with constant density throughout a sphere. However, for a realistic neutron star, its composition is much more complicated than a simple uniform neutron sphere (Lattimer & Prakash 2004). That is, not only neutrons but also protons, leptons and even some non-nucleonic degrees of freedom may appear inside the neutron star. Furthermore, the density profiles for various constituents in the neutron star are far beyond uniformly distributed. These variations could become even more important and interesting when we deal with IVDM which interacts with various components differently. For example, in the extreme case that DM only couples to protons (as for anapole interactions (Fitzpatrick & Zurek 2010; Ho & Scherrer 2013)), constraints on DM-nucleon cross sections set by neutron stars would become much weaker (but non-zero) due to

the fact that the proton fraction is usually much smaller than the neutron fraction inside a typical neutron star.

The motivation of the present work is twofold. Firstly, we investigate how the isospin violating DM-nucleon interactions and the symmetry energy in the equation of state (EOS) of isospin asymmetric nuclear matter affect the extraction of the bound on the DM-proton scattering cross-section σ_p from the existence of old neutron stars, by considering, for the first time, a more realistic neutron star model in which the neutron star is assumed to be static and composed of β -stable and electrically neutral $npe\mu$ matter (i.e., the so-called conventional neutron stars) and its structure is obtained by solving the Tolman-Oppenheimer-Volkoff (TOV) equations. Secondly, we extract the bound on the DM-proton scattering cross-section σ_p from the existence of a realistic isolated pulsar, i.e., the observed nearby old neutron star PSR B1257+12, and compare the results with those from direct detection experiments, especially for IVDM. We restrict our attention on the non-interacting bosonic asymmetric IVDM within the GeV mass region which is favored by recent DM direct detection experiments. Our results indicate that both the isospin violating DM-nucleon interactions and the symmetry energy can significantly affect the extraction of the bound on the DM proton scattering cross-section σ_p from the existence of old neutron stars. In particular, the observed nearby isolated old neutron star PSR B1257+12 can set a stringent limit for low-mass DM particles that reaches a sensitivity beyond the current best limits from direct detection experiments and excludes the DM interpretation of all previously-reported positive experimental results, including the IVDM.

This article is organized as follows. In Sec. 2 we describe the main models and methods used in the present work, including a brief introduction to the symmetry energy and neutron star structure, how to calculate the capture rates of the DM particles onto a structured neutron star and how to determine the conditions for the black hole formation inside neutron stars. In Sec. 3 we give the main results and discussions, including the symmetry energy effects on the global properties of a typical neutron star, the constraints on the DM-proton scattering cross sections for various isospin-violating cases as well as different symmetry energy cases, and the constraints on the DM-proton scattering cross sections from the observed nearby isolated old neutron star PSR B1257+12. We present our conclusions in Sec. 4. An appendix is given to describe the general relativity corrections of DM thermalization and BEC formation in neutron stars.

2. MODELS AND METHODS

2.1. The symmetry energy and neutron star structure

The symmetry energy essentially characterizes the isospin dependent part of the EOS of isospin asymmetric nuclear matter and it is defined via the parabolic approximation to the nucleon specific energy (i.e., EOS) of an asymmetric nuclear matter, i.e.,

$$E(n, \delta) = E_0(n) + E_{\text{sym}}(n)\delta^2 + \mathcal{O}(\delta^4), \quad (1)$$

with baryon density $n = n_p + n_n$ and isospin asymmetry $\delta = (n_n - n_p)/n$ where n_p and n_n denote the proton and neutron densities, respectively. $E_0(n) = E(n, \delta = 0)$ is

the EOS of symmetric nuclear matter, and the symmetry energy can be expressed as

$$E_{\text{sym}}(n) = \frac{1}{2!} \left. \frac{\partial^2 E(n, \delta)}{\partial \delta^2} \right|_{\delta=0}. \quad (2)$$

Because of the exchange symmetry between protons and neutrons (isospin symmetry) in nuclear matter, there are no odd-order δ terms in Eq. (1). The empirical parabolic law in Eq. (1) for EOS of asymmetric nuclear matter has been confirmed by all many-body theory calculations to date, at least for densities up to moderate values (Li et al. 2008).

Around a reference density n_r , the symmetry energy $E_{\text{sym}}(n)$ can be further expanded as

$$E_{\text{sym}}(n) = E_{\text{sym}}(n_r) + \frac{L(n_r)}{3} \left(\frac{n - n_r}{n_r} \right) + \mathcal{O} \left(\frac{n - n_r}{n_r} \right)^2, \quad (3)$$

with the density slope parameter defined as

$$L(n_r) = 3n_r \left. \frac{\partial E_{\text{sym}}(n)}{\partial n} \right|_{n=n_r}. \quad (4)$$

The slope parameter $L(n_r)$ reflects the density dependence of symmetry energy around n_r .

The EOS of isospin asymmetric nuclear matter essentially determines the structure of the conventional neutron stars (see, e.g., Ref. (Xu et al. 2009)). In the present work, the structure of the conventional neutron stars is obtained by solving the TOV equations, i.e.,

$$\frac{dM(r)}{dr} = 4\pi r^2 \epsilon(r) \quad (5)$$

$$\frac{dP(r)}{dr} = -\frac{G\epsilon(r)M(r)}{r^2} \left[1 + \frac{P(r)}{\epsilon(r)} \right] \times \left[1 + \frac{4\pi P(r)r^3}{M(r)} \right] \left[1 - \frac{2GM(r)}{r} \right]^{-1}, \quad (6)$$

where G is Newton's gravitational constant, $M(r)$ is the gravitational mass inside the sphere of radius r , $\epsilon(r)$ and $P(r)$ are, respectively, the corresponding total energy density and total pressure of the neutron star matter at radius r :

$$\epsilon(r) = \epsilon_b(r) + \epsilon_l(r) \quad (7)$$

$$P(r) = P_b(r) + P_l(r). \quad (8)$$

In the present paper, the natural unit $\hbar = c = 1$ is adopted. The neutron star matter is assumed to be neutrino free and only composed of neutrons, protons, electrons and muons in β -equilibrium with charge neutrality (i.e., the $npe\mu$ matter). Thus the baryon part ϵ_b of the total energy density can be written as

$$\epsilon_b(n_b, \delta_{\text{eq}}) = n_b E(n_b, \delta_{\text{eq}}) + m_b n_b, \quad (9)$$

where m_b is the baryon mass, n_b is the local baryon density at the radius r and the local isospin asymmetry δ_{eq} is determined by the β -equilibrium with charge neutrality condition. The energy density of leptons ϵ_l is calculated using the non-interacting Fermi gas model, and can be expressed as:

$$\epsilon_l = \eta \vartheta(\kappa), \quad (10)$$

where η and $\vartheta(\kappa)$ are defined, respectively as

$$\eta = \frac{m_l}{8\pi^2 \lambda^3}$$

$$\vartheta(\kappa) = \kappa \sqrt{1 + \kappa^2} (1 + 2\kappa^2) - \ln \left(\kappa + \sqrt{1 + \kappa^2} \right)$$

with

$$\lambda = \frac{1}{m_l}, \quad \kappa = \lambda(3\pi^2 n_l)^{1/3}.$$

In the above expressions, m_l and n_l are the lepton mass and density, respectively. Then the corresponding pressure can be obtained through the thermodynamical relation:

$$P_i = n_i^2 \frac{d(\epsilon_i/n_i)}{dn_i}, \quad (i = b \text{ or } l). \quad (11)$$

For the $npe\mu$ matter, the β -equilibrium condition is

$$\mu_n - \mu_p = \mu_e = \mu_\mu, \quad (12)$$

where μ_i ($i = n, p, e, \mu$) represents the chemical potential of the particle species i . For neutrons and protons, the chemical potential is determined by the EOS of isospin asymmetric nuclear matter via its definition as

$$\mu_i = \frac{d(nE(n, \delta))}{dn_i}, \quad (i = n \text{ or } p). \quad (13)$$

For leptons (electrons and muons), their chemical potentials can be expressed as

$$\mu_l = \sqrt{p_{Fl}^2 + m_l^2}, \quad (14)$$

where the lepton's Fermi momentum is

$$p_{Fl} = (3\pi^2 n_l)^{1/3}. \quad (15)$$

Eq. (12) together with the charge neutrality condition

$$n_p = n_e + n_\mu \quad (16)$$

then determine the proton fraction $x_p = n_p/n_b$ and the fractions of other particles as functions of baryon density in the neutron star matter.

For the calculations of asymmetric nuclear matter EOS, we use in the present work the standard Skyrme-Hartree-Fock (SHF) approach (see, e.g., Ref. (Chabanat et al. 1997)) in which the nuclear effective interaction is taken to have a zero-range, density- and momentum-dependent form, i.e.,

$$\begin{aligned} V_{12}(\mathbf{R}, \mathbf{r}) = & t_0(1 + x_0 P_\sigma) \delta(\mathbf{r}) \\ & + \frac{1}{6} t_3(1 + x_3 P_\sigma) n^\sigma(\mathbf{R}) \delta(\mathbf{r}) \\ & + \frac{1}{2} t_1(1 + x_1 P_\sigma) [K'^2 \delta(\mathbf{r}) + \delta(\mathbf{r}) K^2] \\ & + t_2(1 + x_2 P_\sigma) \mathbf{K}' \cdot \delta(\mathbf{r}) \mathbf{K} \\ & + i W_0(\sigma_1 + \sigma_2) \cdot [\mathbf{K}' \times \delta(\mathbf{r}) \mathbf{K}], \end{aligned} \quad (17)$$

with $\mathbf{r} = \mathbf{r}_1 - \mathbf{r}_2$ and $\mathbf{R} = (\mathbf{r}_1 + \mathbf{r}_2)/2$. In the above expression, the relative momentum operators $\mathbf{K} = (\nabla_1 - \nabla_2)/2i$ and $\mathbf{K}' = -(\nabla_1 - \nabla_2)/2i$ act on the wave function on the right and left, respectively. The quantities P_σ and σ_i represent, respectively, the spin exchange operator and Pauli spin matrices.

The Skyrme interaction in Eq. (17) includes totally 10 parameters, i.e., the 9 Skyrme force parameters σ , $t_0 - t_3$, $x_0 - x_3$, and the spin-orbit coupling constant W_0 . This standard SHF approach has been shown to be very successful in describing the structure of finite nuclei as well as the properties of neutron stars (Chabanat et al. 1997; Friedrich & Reinhard 1986; Klüpfel et al. 2009).

2.2. DM accretion onto neutron stars

In this work, we consider DM accretion onto neutron stars by following the basic lines of Refs. (Press & Spergel 1985; Gould 1987; Kouvaris 2008). We suppose that the neutron star seizes DM particles from the area locating on a sphere of radius R_0 centered at the center of the neutron star. We further let $R_0 \rightarrow \infty$, which means that R_0 is so large that the gravitational field of the neutron star at $r = R_0$ is negligible. We further assume that the neutron star is motionless with respect to the ambient DM halo and thus a spherically symmetric accretion scenario is adopted. Then the flux of DM crossing the spherical surface (per unit time) with velocity ranging from v to $v + dv$ and the angle relative to the normal line between α and $\alpha + d\alpha$ is

$$dF = p(v)dv v \cos \alpha \sin \alpha 2\pi R_0^2 d\alpha, \quad (18)$$

where $p(v)$ is the local DM velocity distribution evaluated in the Galactic rest frame and α is limited within the region $[\frac{\pi}{2}, \pi]$ to ensure that only the DM particles moving toward the neutron star are available for accretion. Integrating dF with respect to v and α , one can get the maximum number of DM particles which are possible to be captured by the neutron star. In order to determine the integrating phase space for each variable, we first study the trajectory for a non-relativistic DM particle traveling outside the neutron star which is given by the so-called geodesic equation

$$\frac{A(r)}{r^4} \left(\frac{dr}{d\varphi} \right)^2 + \frac{1}{r^2} - \frac{1}{J^2 B(r)} = -\frac{e}{J^2}. \quad (19)$$

Here r and φ are the polar coordinates and without loss of generality, the motion of the DM particle is taken to be in the $\theta = \pi/2$ plane. $A(r)$ and $B(r)$ are the space-time geometry of a spherically symmetric system defined by

$$ds^2 = -B(r)dt^2 + A(r)dr^2 + r^2 d\theta^2 + r^2 \sin^2 \theta d\varphi^2, \quad (20)$$

and their values are affected by the energy distribution of the whole system. In the vacuum outside the neutron star, we have $A(r) = (1 - \frac{2GM_S}{r})^{-1}$ and $B(r) = A^{-1}$ which are known as the Schwarzschild metrics and are uniquely determined by the neutron star mass M_S divided by the radial distance from the center point, i.e. M_S/r . Moreover, in Eq. (19), the angular momentum per unit mass J and the variable e are defined as

$$J = vR_0 \sin \alpha, \quad (21)$$

$$e = 1 - 2E_0, \quad (22)$$

with $E_0 = \frac{1}{2}v^2$ being the total energy per unit mass at $r = R_0$. It should be noted that both J and e are defined at $r = R_0$, and they are invariant integrals of orbits both in- and outside the neutron star due to the conservation

of angular momentum and energy. We consider the fact that the DM particles can be captured by the neutron stars only if they are able to interact with the neutron star matter. That is to say, the allowed variable regions for the variables in Eq. (18), which ensure that the traveling trajectories of the DM particles pass through the neutron star for capturing, can be obtained equivalently by requiring that the perihelion radius (closest distance to the center of the neutron star), r_p , for each particle must be less than or equal to the neutron star radius, R_S . The perihelion radius r_p can be obtained by letting

$$\left. \frac{dr}{d\varphi} \right|_{r=r_p} = 0 \quad (23)$$

in Eq. (19), and the requirement $r_p \leq R_S$ leads to the following condition for capturing

$$J^2 \leq J_M^2 = R_S^2 \left[\left(1 - \frac{2GM_S}{R_S} \right)^{-1} - e \right]. \quad (24)$$

So it is more convenient to express Eq. (18) in terms of J and E_0 according to their relationship with respect to v and α mentioned previously. Furthermore, we assume that the DM population in the DM halo follows a Maxwell-Boltzmann distribution of velocities in the Standard Halo Model, that is,

$$p(v)dv = n_\chi \left(\frac{1}{\pi v_0^2} \right)^{3/2} 4\pi v^2 e^{-\frac{v^2}{v_0^2}} dv, \quad (25)$$

where n_χ is the DM number density of the DM halo around the neutron star, and v_0 is the most probable speed of the velocity distribution. Then Eq. (18) can be re-expressed as

$$dF = n_\chi \left(\frac{1}{\pi v_0^2} \right)^{3/2} 4\pi^2 e^{-\frac{2E_0}{v_0^2}} dE_0 dJ^2, \quad (26)$$

and the total capture rate of the DM particles can be obtained as

$$\begin{aligned} F &= \int_0^\infty \int_0^{J_M^2} dF \\ &= n_\chi \left(\frac{1}{\pi v_0^2} \right)^{\frac{3}{2}} 4\pi^2 R_S^2 \frac{v_0^2}{2} \left[\left(1 - \frac{2GM_S}{R_S} \right)^{-1} - 1 \right], \end{aligned} \quad (27)$$

where we integrate over E_0 from zero to infinity and over J^2 from zero to J_M^2 according to Eq. (24).

2.3. DM scattering with neutron star matter

In order to be trapped by a neutron star, the DM particles are required to scatter with the neutron star matter and lose enough energy to form some bound orbits. Since the velocities of the DM particles approaching the surface of the neutron star are roughly equal to the local escape velocity ($\sim 0.6c$), even one collision is enough to ensure such a bound orbit. The fraction that the DM particles undergo at least one collision inside the neutron star can be expressed as (Kouvaris 2008)

$$f = \left\langle 1 - e^{-\int \sigma_\chi n_b dt} \right\rangle, \quad (28)$$

where the angle brackets represent the average over all possible DM trajectories in the above equation, and n_b is the local baryon number density, σ_χ denotes the effective scattering cross section between the DM particles and nucleons inside the neutron star.

For a conventional neutron star consisting only of nucleons and leptons as we are considering in the present work, σ_χ can be evaluated in terms of the DM-proton and DM-neutron scattering cross sections in infinite nuclear matter as

$$\begin{aligned}\sigma_\chi &= \sigma_p \xi_p(r) x_p(r) + \sigma_n \xi_n(r) [1 - x_p(r)] \\ &= \sigma_p [g_{np}^2 \xi_n + (\xi_p - g_{np}^2 \xi_n) x_p].\end{aligned}\quad (29)$$

Here $\sigma_{p,n}$ denote the DM-proton and DM-neutron cross sections in free space, respectively. g_{np} is the so-called isospin-violating factor which is defined as

$$g_{np} = \frac{f_n}{f_p}, \quad (30)$$

with $f_{n,p}$ denoting the effective coupling of DM to neutrons and protons, respectively. The factor $\xi_{p,n}$ takes into account the medium corrections on the DM-nucleon scattering cross sections by considering the Pauli blocking and Fermi motion due to the proton (neutron) degeneracy effect and it can be analytically expressed as (Chen et al. 2001)

$$\xi_{p,n} = 1 - \frac{2}{5} \left(\frac{p_F^{p,n}}{p_\chi} \right)^2, \quad (31)$$

for $p_\chi > p_F^{p,n}$, and it becomes

$$\begin{aligned}\xi_{p,n} &= 1 - \frac{2}{5} \left(\frac{p_F^{p,n}}{p_\chi} \right)^2 \\ &+ \frac{2}{5} \left(\frac{p_F^{p,n}}{p_\chi} \right)^2 \left[1 - \left(\frac{p_\chi}{p_F^{p,n}} \right)^2 \right]^{5/2},\end{aligned}\quad (32)$$

for $p_\chi < p_F^{p,n}$. Here $p_\chi = m_\chi \frac{v_{\text{esc}}}{\sqrt{1 - v_{\text{esc}}^2}}$ is the momentum of the incident DM particle with $v_{\text{esc}} = \sqrt{1 - B(r)}$ (Lavallaz & Fairbairn 2010) denoting the local escape velocity of the neutron star, and the Fermi momenta are given by $p_F^{p,n} = (3\pi^2 n_{p,n})^{1/3}$. We ignore the scattering between the DM particles and leptons since the masses of leptons possibly existing inside the neutron stars, e.g., $m_e \sim 0.5$ MeV and $m_\mu \sim 100$ MeV, are much smaller than the DM mass we are interested in here (~ 10 GeV), and the scattering with these light leptons would hardly affect the motion of the DM particles.

In Eq. (28), the arc length along an orbit, dl , is given by

$$\begin{aligned}dl &= \sqrt{A(r)dr^2 + r^2 d\varphi^2} \\ &= d\varphi \frac{r^2}{\sqrt{J^2}} \sqrt{\frac{1}{B(r)} - e}.\end{aligned}\quad (33)$$

where we have already applied the geodesic equation (Eq. (19)) to obtain the expression in the second line. Similarly, we have also taken the calculation within the $\theta = \pi/2$ plane. We would like to emphasize here that the

metric in front of dr^2 in Eq. (33) now has the following form, that is,

$$A(r) = \left(1 - \frac{2GM(r)}{r} \right)^{-1}, \quad (34)$$

where $M(r)$ is the gravitational mass within the radius r instead of the mass of the whole neutron star as that in Eq. (20). Similarly, the metric in front of the time, $B(r)$, in Eq. (33) is now given by

$$B(r) = e^{2\phi(r)} \quad (35)$$

with

$$\phi(r) = - \int_r^\infty \frac{G}{r'^2} \frac{M(r') + 4\pi r'^3 P(r')}{1 - \frac{2GM(r')}{r'}} dr'. \quad (36)$$

Here the $\phi(r)$ corresponds to an effective Newton-like gravitational potential (see the appendix) which is used to determine the black hole formation conditions in the next subsection. The integrating limit in Eq. (36) is from r to infinity, and one can easily verify that Eq. (35) returns back to the Schwarzschild-like form as that in Eq. (20) when the radius $r > R_S$.

Finally, in Eq. (28), for a given neutron star, we average over all the possible paths of the DM particles passing through the neutron star. Since the traveling trajectories of the DM particles are fixed by the initial conditions of motion at $r = R_0$, Eq. (28) can be further expressed according to the DM population distribution at R_0 as

$$f = \langle Q \rangle = \frac{\int_0^\infty dv \int_0^{\alpha_M} d\alpha p(v) q(\alpha) Q}{\int_0^\infty dv \int_0^{\alpha_M} d\alpha p(v) q(\alpha)}, \quad (37)$$

where we have $Q = 1 - e^{-\int \sigma_\chi n_b dl}$, and $p(v)$ and $q(\alpha)$ are the velocity distribution and angular distribution of ambient DM halo, respectively. Since we are interested in the isotropic case, the angular distribution can be reduced to $q(\alpha) = 1$. According to the discussions about Eq. (18) and Eq. (26) in the previous subsection, it will be more convenient to express Eq. (37) in terms of J and E_0 rather than v and α . Thus the limit of the angular integration, α_M , corresponds to J_M we introduced previously according to the relation $J_M = v R_0 \sin \alpha_M$ (see, Eq. (21)), and the integration over E_0 remains from 0 to ∞ . Once again, by assuming that the DM population follows a Maxwell-Boltzmann distribution for velocities as in Eq. (25), we can re-express Eq. (37) as

$$\begin{aligned}f &= \frac{\int_0^\infty e^{-\frac{2E_0}{v_0^2}} dE_0 \int_0^{J_M^2} \left(1 - \frac{J^2}{2E_0 R_0^2} \right)^{-1/2} \frac{Q(J^2, E_0)}{\sqrt{J^2}} dJ^2}{\int_0^\infty e^{-\frac{2E_0}{v_0^2}} dE_0 \int_0^{J_M^2} \left(1 - \frac{J^2}{2E_0 R_0^2} \right)^{-1/2} \frac{1}{\sqrt{J^2}} dJ^2} \\ &\approx \frac{\int_0^{J_M^2} \frac{Q(J^2)}{\sqrt{J^2}} dJ^2}{2\sqrt{J_M^2}}.\end{aligned}\quad (38)$$

We have assumed $\left(1 - \frac{J^2}{2E_0 R_0^2} \right)^{-1/2} \approx 1$ and $e \approx 1$ in order to simplify the expression to the form given in the second line in Eq. (38), and these approximations are always valid for all cases satisfying $R_0 \rightarrow \infty$.

Combining Eq. (27) and Eq. (38) together, we can get the total mass M_t of the DM particles that can be trapped by a neutron star in a period of time t as

$$M_t = 4.07 \times 10^{40} \text{ GeV} \frac{M_S R_S}{1 - 2.964 \frac{M_S}{R_S}} \left(\frac{m_\chi n_\chi}{0.3 \text{ GeV/cm}^3} \right) \times \left(\frac{v_0}{220 \text{ km/s}} \right)^{-1} \left(\frac{t}{\text{Gyr}} \right) f, \quad (39)$$

where M_S is the gravitational mass of the neutron star in unit of solar mass M_\odot and R_S is neutron star radius in unit of km. It should be noted here that the structure effects of neutron stars on M_t are due to the factor f .

We would like to point out that all the expressions above have been obtained within the framework of general relativity. And for Newtonian case, we note that the trapped mass of the DM particles will be reduced by about a factor of 2.

2.4. Black hole formation and neutron star destruction

Since we focus on the non-interacting bosonic ADM in the present work, the Chandrasekhar limit of the mass for a boson star consisting of such kind of DM can be expressed as (Kouvaris & Tinyakov 2011; Bramante et al. 2013)

$$M_{\text{cha}} = \frac{2}{\pi} \frac{M_{\text{pl}}^2}{m_\chi}, \quad (40)$$

where $M_{\text{pl}} = 1.22 \times 10^{19} \text{ GeV}$ is the Planck mass.

After being captured by the neutron star, a DM particle will go on scattering with the neutron star matter until its velocity reduces to the thermal velocity depending on the local temperature of the neutron star matter. The spending time of this thermalization process has been estimated by Kouvaris in Ref. (Kouvaris 2013), and it can be parameterized as

$$t_{\text{th}} = 0.2 \text{ yr} \left(\frac{m_\chi}{\text{TeV}} \right)^2 \left(\frac{\sigma_\chi}{10^{-43} \text{ cm}^2} \right)^{-1} \left(\frac{T}{10^5 \text{ K}} \right)^{-1}, \quad (41)$$

which agrees with the vast majority of results given by other authors (McDermott et al. 2012; Bramante et al. 2013; Bertoni et al. 2013). The value of t_{th} is much smaller than the living age of the old neutron stars we are interested in. Therefore one can assume that the DM particles are totally thermalized as soon as they are captured by the neutron star. Thermalized DM particles will continually drift to the neutron star center and accumulate within a typical thermal radius,

$$r_{\text{th}} = \left[\frac{9T_c}{4\pi G m_\chi B_0(\epsilon_c + 3P_c)} \right]^{1/2} \approx 2.2 \text{ m} \left[\frac{\text{GeV}}{m_\chi} \frac{T_c}{10^5 \text{ K}} \frac{\text{GeV} \cdot \text{fm}^{-3}}{B_0(\epsilon_c + 3P_c)} \right]^{1/2}, \quad (42)$$

where $B_0 = B(0)$ (see Eq. (35)), m_N denotes the mass of nucleons, and T_c , ϵ_c and P_c are the temperature, energy density and pressure at the center of the neutron star, respectively. Derivation of Eq. (42) takes into account the correction of general relativity as detailed in the appendix. Once the gravity of the accumulated DM

particles exceeds that of the baryons (the corresponding critical number of DM particles is $N_{\text{th}}^{\text{self}} = 4\pi r_{\text{th}}^3 n_c/3$ where n_c is the baryon density at the neutron star center), the self-gravitation will take place so that the DM particles can form a boson star at the center of the host neutron star. For $m_\chi \leq 10^{17} \text{ GeV} (T_c/10^5 \text{ K})^3$ which is always satisfied in the cases we are considering here, the boson star mass is larger than the Chandrasekhar limit M_{cha} (see, e.g., Ref. (McDermott et al. 2012)), and thus the gravitational collapse always occurs as soon as these thermalized DM particles become self-gravitating in the neutron star.

In the above discussion, the thermalized DM particles have been assumed to follow a Maxwellian velocity distribution. However, for the non-interacting bosonic DM system with extremely high density, the formation of a macroscopic quantum state, i.e., BEC, confined by the neutron star's gravitational field, can take place when the number of the thermalized DM particles exceeds (see the appendix)

$$N_{\text{BEC}} = \zeta(3) \left[\frac{T_c}{\sqrt{4\pi G B_0(\epsilon_c + 3P_c)}/3} \right]^3 \approx 2.4 \times 10^{35} \left(\frac{T_c}{10^5 \text{ K}} \right)^3 \left[\frac{\text{GeV} \cdot \text{fm}^{-3}}{B_0(\epsilon_c + 3P_c)} \right]^{\frac{3}{2}} \quad (43)$$

where $\zeta(3) = 1.202$ is the Riemann zeta function. This condensation process happens always before the occurrence of the self-gravitation of the thermalized DM system for DM roughly lighter than several TeV depending on the temperature of the neutron star core (McDermott et al. 2012; Kouvaris 2013) since we have $N_{\text{BEC}} < N_{\text{th}}^{\text{self}}$. The DM particles which exceed N_{BEC} will lose their kinetic energy and go to the ground state. Being attracted by the neutron star's gravity, they will gather within a radius (see the appendix)

$$r_{\text{BEC}} = \left[\frac{3}{8\pi G m_\chi^2 B_0(\epsilon_c + 3P_c)} \right]^{1/4} \approx 1.4 \times 10^{-6} \text{ m} \times \left(\frac{\text{GeV}}{m_\chi} \right)^{1/2} \left[\frac{\text{GeV} \cdot \text{fm}^{-3}}{B_0(\epsilon_c + 3P_c)} \right]^{\frac{1}{4}} \quad (44)$$

which is much smaller than the thermal radius given in Eq. (42). In this case, the total mass of the DM particles in the BEC phase required to form self-gravitating system is

$$M_{\text{self}}^{\text{BEC}} \sim m_N n_c \frac{4}{3} \pi r_{\text{BEC}}^3 \approx 10^{28} \text{ GeV} \left(\frac{n_c}{\text{fm}^{-3}} \right) \left(\frac{\text{GeV}}{m_\chi} \right)^{\frac{3}{2}} \left[\frac{\text{GeV} \cdot \text{fm}^{-3}}{B_0(\epsilon_c + 3P_c)} \right]^{\frac{3}{4}}. \quad (45)$$

Assuming $T_c = 10^5 \text{ K}$, $n_c \sim 1 \text{ fm}^{-3}$ and $B_0(\epsilon_c + 3P_c) \sim 0.3 \text{ GeV} \cdot \text{fm}^{-3}$, we note that $M_{\text{self}}^{\text{BEC}} < M_{\text{cha}}$ means $m_\chi > 8 \times 10^{-20} \text{ GeV}$. Therefore, different from the case without considering BEC, for DM with mass $m_\chi \sim \text{GeV}$, they will first form BEC state, and the DM particles in the BEC phase then quickly become self-gravitating to form

a mini boson star which then collapses into black hole as long as the accumulated total DM mass satisfies

$$M_t > M_{\text{cha}} + m_\chi N_{\text{BEC}}. \quad (46)$$

For DM with mass $m_\chi \sim \text{GeV}$ as we are considering in the present work, the mini boson star with DM in BEC state will generally collapse into black hole before the gravitational collapse of the boson star formed directly from thermalized DM particles without considering BEC. Therefore, Eq. (46) determines the condition of black hole formation in the present work.

After black hole formation, the fate of the black hole is then determined by the competition between the black hole accretion and the Hawking radiation. If the black hole first evaporates through Hawking radiation, there will be few observable consequences one can detect, thus one can hardly place any constraints on the DM interactions from the observations of neutron stars. In particular, the growth of the black hole is governed by the equation

$$\frac{dM_{\text{BH}}}{dt} = \frac{4\pi\lambda_s m_N n_c (GM_{\text{BH}})^2}{c_\infty^3} + \left. \frac{dM_{\text{BH}}}{dt} \right|_{\text{DM}} - \frac{1}{15360\pi(GM_{\text{BH}})^2}, \quad (47)$$

where M_{BH} is the black hole mass which equals to the critical mass M_{cha} at $t = 0$. The first term on the right hand side of Eq. (47) denotes the accretion rate of the neutron star matter by the black hole, and a spherically symmetric Bondi accretion scenario is adopted for this term in the present work. The term $\left. \frac{dM_{\text{BH}}}{dt} \right|_{\text{DM}}$ is the accretion rate of the DM particles by the black hole, and for DM which has already formed a BEC, its value equals to the DM capture rate by the neutron star (Bramante et al. 2013). The last term represents the Hawking radiation which stalls the growth of the black hole inside the neutron star.

In order to specify the parameters in Eq. (47), we follow the derivation based on relativistic equations for the spherical accretion onto a black hole adopted in Ref. (Shapiro & Teukolsky 1983). To simplify the calculation, we first parameterize the EOS of the neutron star matter for $n_b > n_c$ with a polytropic form as

$$P = K n_b^\Gamma, \quad (48)$$

where P is the pressure of the neutron star matter, and K and Γ are constant parameters. In this case, the non-dimensional accretion parameter λ_s in the first term on the right hand side of Eq. (47) can then be given by

$$\lambda_s = \frac{1}{4} \left(\frac{c_s}{c_\infty} \right)^{\frac{5-3\Gamma}{\Gamma-1}} (1 + 3c_s^2)^{\frac{3\Gamma-2}{2\Gamma-2}}, \quad (49)$$

where c_∞ , also appearing in the first term on the right hand side of Eq. (47), is the neutron star matter sound speed at the center of the neutron star which can be obtained according to its definition as

$$c_\infty^2(n_c) \equiv \left. \frac{dP}{d\epsilon} \right|_{n_b=n_c} \quad (50)$$

with ϵ being the energy density of the neutron star matter. In Eq. (49), the sound speed at the sonic point c_s

corresponding to c_∞ is given by the relation

$$(1 + 3c_s^2) \left(1 - \frac{c_s^2}{\Gamma - 1} \right)^2 = \left(1 - \frac{c_\infty^2}{\Gamma - 1} \right)^2. \quad (51)$$

Here the sonic point is known as the “critical point” where the radial velocity of the accreting flows becomes equal to the sound speed in the neutron star matter.

As one can see from Eq. (47), the Bondi accretion rate is proportional to the square of the black hole mass while the Hawking radiation rate is proportional to the inverse of the squared black hole mass. In addition, the DM accretion rate is independent of M_{BH} and can be set as a constant throughout the calculation. This implies that the black hole will go on growing and eventually destroy the host neutron star if its initial mass is large enough to ensure

$$\left. \frac{dM_{\text{BH}}}{dt} \right|_{t=0} > 0, \quad (52)$$

otherwise it will evaporate through Hawking radiation firstly in return.

Therefore, the fact that old neutron stars do exist in our Galaxy indicates that we must have either $M_t < M_{\text{cha}} + m_\chi N_{\text{BEC}}$ or $\left. \frac{dM_{\text{BH}}}{dt} \right|_{t=0} < 0$ to prevent the destruction of neutron stars, and this will put strong constraints on the scattering cross sections between DM particles and nucleons in neutron stars. In particular, by introducing the isospin-violating DM in our calculations, we can thus constrain the isospin-dependent scattering properties between this kind of DM and the nucleons inside neutron stars.

3. RESULTS AND DISCUSSIONS

3.1. Nuclear symmetry energy effects on the structure of neutron stars

In order to obtain the constraints on DM properties from neutron stars, we should first figure out the structure of the host neutron star. Specifically, the EOS of isospin asymmetric nuclear matter is a basic ingredient to determine the properties of neutron stars as discussed earlier. While for symmetric nuclear matter with equal fractions of neutrons and protons, its EOS $E_0(n)$ is relatively well determined, the EOS of asymmetric nuclear matter, especially the density dependence of the nuclear symmetry energy, $E_{\text{sym}}(n)$, is largely unknown (Li et al. 2008). In particular, although the nuclear symmetry energy at the subsaturation cross density $n_{\text{cross}} \approx 0.11 \text{ fm}^{-3}$ is known to be around 26.65 MeV from a recent work by analyzing the binding energy difference of a number of heavy isotope pairs (Zhang & Chen 2013), its values at other densities, especially at supra-saturation densities, are still poorly known.

Shown in Fig. 1 is the nuclear symmetry energy $E_{\text{sym}}(n)$ as a function of baryon density in SHF calculations with 2 Skyrme interactions, i.e., MSL1 and Lc92 (Zhang & Chen 2013; Zheng et al. 2014). These two interactions are based on the modified Skyrme-like (MSL) model (Chen et al. 2010; Zhang & Chen 2013; Chen 2011; Chen & Gu 2012; Chen 2011) in which the 9 Skyrme interaction parameters σ , $t_0 - t_3$, $x_0 - x_3$ are expressed analytically in terms of 9 macroscopic quantities, i.e., the saturation density n_0 , $E_0(n_0)$, the incompressibility K_0 , the isoscalar effective mass $m_{s,0}^*$, the

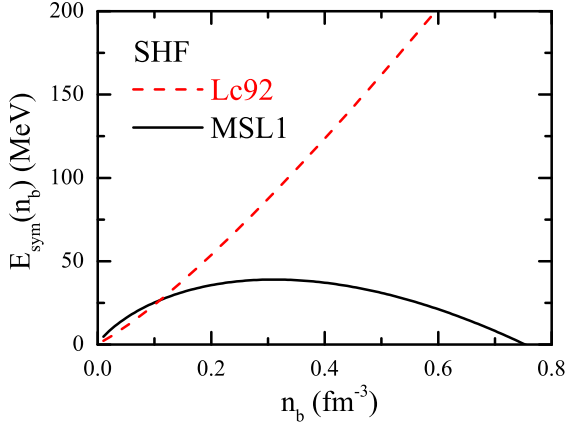


FIG. 1.— (Color online) Density dependence of the symmetry energy in the SHF model with MSL1 and Lc92.

TABLE 1
PARAMETERS OF THE SKYRME FORCES MSL1 AND Lc92.

	MSL1	Lc92
t_0 (MeV \cdot fm ³)	-1963.23	-1962.93
t_1 (MeV \cdot fm ⁵)	379.845	379.795
t_2 (MeV \cdot fm ⁵)	-394.554	-394.798
t_3 (MeV \cdot fm ^{3+3σ})	12174.9	12174.3
x_0	0.32077	-0.73832
x_1	0.344849	0.344954
x_2	-0.847304	-0.84731
x_3	0.32193	-1.5352
σ	0.26936	0.26942
W_0 (MeV \cdot fm ⁵)	113.62	113.62

isovector effective mass $m_{v,0}^*$, $E_{\text{sym}}(n_r)$ at a reference density n_r , the slope parameter of the symmetry energy $L(n_r)$, G_S , and G_V . The G_S and G_V are respectively the gradient and symmetry-gradient coefficients in the interaction part of the binding energies for finite nuclei. Specifically, the MSL1 interaction (Zhang & Chen 2013) has been obtained by fitting a number of experimental data of finite nuclei, including the binding energy, the charge rms radius, the neutron $3p_{1/2} - 3p_{3/2}$ energy level splitting in ^{208}Pb , isotope binding energy difference, and neutron skin data of Sn isotopes. The Lc92 interaction has been obtained by setting $L(n_{\text{cross}}) = 92.4$ MeV in the MSL1 interaction to fit the latest model-independent measurement of the neutron skin thickness of ^{208}Pb from PREX experiment at JLab (Abrahamyan et al. 2012) while keeping the other 8 macroscopic quantities and the spin-orbit coupling constant W_0 fixed at their default values in the MSL1 interaction. The corresponding Skyrme force parameters of these two interactions are listed in Table 1. We have selected these two interactions in such a way that they give good descriptions for the properties of finite nuclei (Zhang & Chen 2013; Zheng et al. 2014) while predict totally different behaviors of $E_{\text{sym}}(n)$ at supra-saturation densities as shown in Fig. 1 which essentially represent the current uncertainties of the high density behaviors of the symmetry energy.

The global properties of static neutron stars are determined by the EOS of neutron star matter over a broad density region ranging from the center to the surface of neutron stars. Generally, a typical neutron star contains the liquid core, inner crust, and outer crust from the

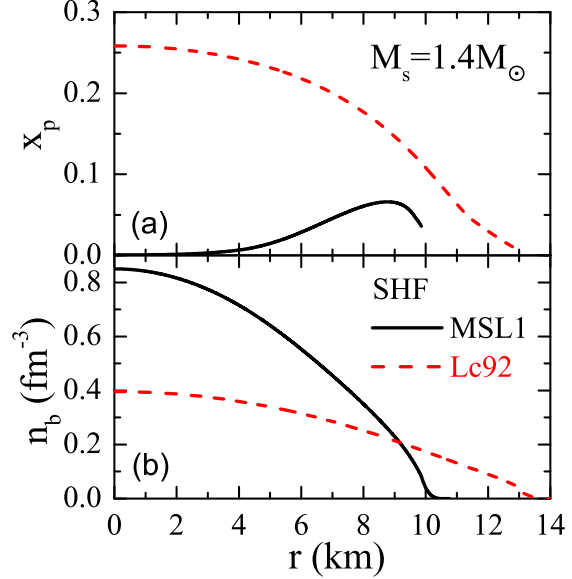


FIG. 2.— (Color online) Proton fraction in the homogeneous liquid core (upper panel) and baryon number density (lower panel) as functions of the radius r inside a typical neutron star with mass of $1.4 M_\odot$ from SHF model with MSL1 (solid lines) and Lc92 (dashed lines).

center to surface. For the liquid core, we use the EOS of $npe\mu$ matter from SHF calculations introduced earlier. In the inner crust with densities between n_{out} and the transition density n_t where the nuclear pastas may exist, because of our poor knowledge about its EOS from first principle, following Carriere *et al.* (Carriere et al. 2003) (see also Refs. (Xu et al. 2009; Zheng & Chen 2012)) we construct its EOS according to

$$P = a + b\epsilon^{4/3}. \quad (53)$$

This polytropic form with an index of $4/3$ has been found to be a good approximation to the crust EOS (Lattimer & Prakash 2000, 2001; Link et al. 1999). The $n_{\text{out}} = 2.46 \times 10^{-4} \text{ fm}^{-3}$ is the density separating the inner from the outer crust. The core-crust transition density n_t of neutron stars is determined self-consistently with the Skyrme interactions by a dynamical approach (See Refs. (Xu et al. 2009; Zheng & Chen 2012) for details). The constants a and b are then determined by

$$a = \frac{P_{\text{out}}\epsilon_t^{4/3} - P_t\epsilon_{\text{out}}^{4/3}}{\epsilon_t^{4/3} - \epsilon_{\text{out}}^{4/3}}, \quad (54)$$

and

$$b = \frac{P_t - P_{\text{out}}}{\epsilon_t^{4/3} - \epsilon_{\text{out}}^{4/3}}, \quad (55)$$

where P_t (ϵ_t) and P_{out} (ϵ_{out}) are the pressure (energy density) at n_t and n_{out} , respectively. In the outer crust with $6.93 \times 10^{-13} \text{ fm}^{-3} < n < n_{\text{out}}$, we use the EOS of BPS (Baym et al. 1971; Iida & Sato 1997), and in the region of $4.73 \times 10^{-15} \text{ fm}^{-3} < n < 6.93 \times 10^{-13} \text{ fm}^{-3}$ we use the EOS of Feynman-Metropolis-Teller (Baym et al. 1971).

Using the EOS constructed above, one can solve the TOV equations (Eq. (6)) to obtain the global properties of static neutron stars. In the upper panel of Fig. 2, we

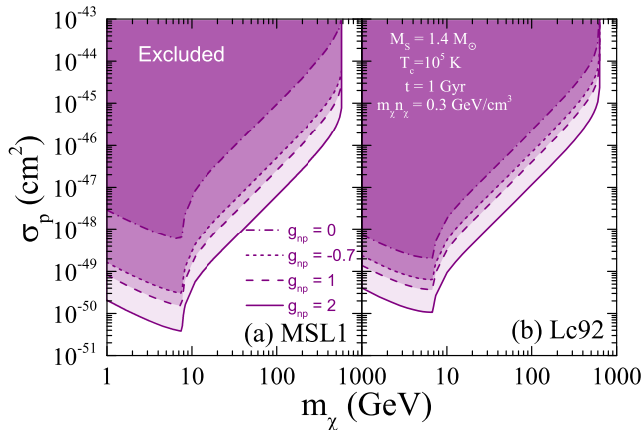


FIG. 3.— (Color online) Exclusion contour in m_χ - σ_p plane for the non-interacting bosonic asymmetric IVDM from a typical neutron star with $M_S = 1.4M_\odot$, $T_c = 10^5$ K, $t = 1$ Gyr and $m_\chi n_\chi = 0.3$ GeV/cm³ within SHF model with MSL1 (a) and Lc92 (b) for $g_{np} = 0, -0.7, 1$ and 2 .

show the proton fraction in the homogeneous liquid core inside the neutron star as a function of the radius r for a typical neutron star with mass of $1.4 M_\odot$ by using MSL1 and Lc92. It is interesting to see that different Skyrme interactions predict totally different proton distributions inside the liquid core of the neutron star. In particular, for the MSL1 interaction which predicts a very soft symmetry energy as shown in Fig. 1, it is suggested that the neutron star core is almost comprised of pure neutron matter. This feature can be understood from the fact that the symmetry energy predicted by MSL1 reduces to zero or even becomes negative at high density region (see Fig. 1) which will lead to small or even vanishing proton fraction due to β -stability and charge neutrality conditions (see, e.g., Ref. (Xu et al. 2009) and Section 2.1). On the other hand, for Lc92 which predicts increasing relationship between $E_{\text{sym}}(n)$ and n as shown in Fig. 1, large proton fraction is obtained in the neutron star core. Therefore, these results indicate that the neutron and proton compositions inside neutron stars depend strongly on the density dependence of the symmetry energy.

Furthermore, we show the corresponding radial distributions of the baryon number density in the lower panel of Fig. 2. Different from the cases of x_p , the shapes of the curves are qualitatively the same for these two interactions. However, a harder symmetry energy (i.e., Lc92) tends to predict a larger radius of the neutron star and correspondingly a smaller central density in order to keep the neutron star mass remaining the same. In addition, we note that the pressure predicted by different Skyrme interactions exhibits similar radial distribution as the corresponding $n_b(r)$ inside the neutron star. It should be mentioned that x_p , n_b and the pressure P all are needed to calculate the “efficiency” factor f in Eq. (28), and their variations shown in Fig. 2 could lead to significant symmetry energy effects on the constraints on the scattering cross sections between DM and nucleons which we will detail below.

3.2. Effects of isospin-violating interaction and the symmetry energy on the σ_p bounds from old neutron stars

TABLE 2
QUANTITIES USED FOR BLACK HOLE ACCRETION FOR MSL1 AND Lc92.

	MSL1	Lc92
Γ	2.546	2.600
c_∞	0.634	0.517
c_s	0.983	0.954
λ_s	1.415	0.929

For the first time, owing to the consideration of the realistic neutron star model, we are able to investigate the constraint on σ_p for non-interacting bosonic asymmetric IVDM from the existence of old neutron stars. In this subsection, we focus on the effects of isospin-violating interaction and the symmetry energy. If the captured DM particles do form a BEC inside the neutron star, the bounds on σ_p can be obtained by requesting Eq. (46) and Eq. (52) to be satisfied simultaneously. Since both IVDM and ADM are typically modeled in the GeV mass region, in this work, we restrict our interests in DM with mass ranging from 1 GeV to 1 TeV where a number of discoveries and constraints have been claimed or placed by the direct detection experiments. We first list in Table 2 the values of the parameters Γ , c_∞ , c_s and λ_s for MSL1 and Lc92, which are needed to calculate the black hole evolution.

Shown in Fig. 3 is the exclusion contour in the m_χ - σ_p plane obtained by using the fiducial neutron star parameters with a mass of $M_S = 1.4M_\odot$, a living age $t = 1$ Gyr and core temperature $T_c = 10^5$ K (Lattimer & Prakash 2004; Kouvaris 2008; Gonzalez & Reisenegger 2010). Neutron stars with heavier mass and longer age can accrete more DM particles, thus more stringent constraints will be set through Eq. (39). On the other hand, the higher is the core temperature, the more DM particles are required for gravitational collapse (see Eqs. (43) and (46)). In particular, since one has $N_{\text{BEC}} \sim T_c^3$ according to Eq. (46), the constraints will be weakened drastically when the core temperature becomes higher. For neutron stars which are not far from the earth, we use the standard astrophysical parameters in the Standard Halo Model for DM halo, namely, a Maxwell-Boltzmann distribution for $p(v)$ with $v_0 = 220$ km/s and a DM mass density of $m_\chi n_\chi = 0.3$ GeV/cm³ (Smith et al. 2007) in our calculations. Since the scattering process happening inside the neutron star is independent of the DM halo properties and the capture rate depends on n_χ and v_0 simply through the factor n_χ/v_0 (see Eq. (39)), variation of the DM halo properties just rescales the bound on σ_p according to n_χ/v_0 directly. Additionally, although DM should be, in principle, trapped using a combination of scattering in both the core and the crust of the neutron star, for DM first approaching to the neutron stars with high energy, it can scatter efficiently in the core but inefficiently in the crust due to the low matter density as well as the coherent DM-nucleus scattering inside the crust (Horowitz 2012). Therefore, in Fig. 3, we have ignored the scattering occurred inside the neutron star crust when we calculate the capture rate from Eq. (28) and Eq. (39).

It should be noted that in Fig. 3, there exists a bending point around several GeV mass region at which the Hawking radiation rate starts to dominate the inequal-

ities Eqs. (46) and (52). That is, while bounds are obtained from the black hole formation condition presented by Eq. (46) for lighter DM particles (on the left of the bending point), for heavier DM (on the right of the bending point), a larger σ_p (i.e., a larger capture rate of DM) is required to ensure the growth of the black hole according to the evolution function Eq. (47). In addition, the cut-off mass lines around several hundred GeV in Fig. 3 imply that the neutron star is unable to constrain DM heavier than the cut-off mass since the Hawking radiation rate will be always stronger than the accretion rate in Eq. (47) for these heavy DM particles. It is interesting to see that, by taking into account the more realistic EOSs in the calculation for the black hole evolution, the location of the bending point (i.e., 7.43 GeV for MSL1 and 6.44 GeV for Lc92) reduces significantly compared with the values obtained by some other researchers, e.g. 16 GeV in Ref. (Kouvaris & Tinyakov 2011) and 13 GeV in Ref. (McDermott et al. 2012). Our results thus suggest that the location of the bending point depends significantly on the EOS of the neutron star matter.

Moreover, one can see from Fig. 3 that the introduction of isospin-violating interaction could significantly affect the bounds on the σ_p . For instance, in the case of $g_{np} = 0$, which means that DM will only scatter with the protons inside the neutron star, bounds on σ_p would be weakened by more than an order of magnitude relative to the normal case with $g_{np} = 1$. On the other hand, a larger g_{np} (e.g., $g_{np} = 2$) could in turn strengthen the bounds apparently. Bounds on σ_p for IVDM with $g_{np} = -0.7$ are also included in Fig. 3. This g_{np} value was firstly suggested by Feng *et al.* (Feng et al. 2011), and it leads to nearly complete destructive interference of the scattering amplitudes for DM-proton and DM-neutron collisions for xenon-based detectors in the terrestrial direct detection experiments, and has been successfully applied to ameliorate the tension between CDMS-II(Si) and other experiments such as LUX and SuperCDMS (see, e.g., Ref. (Zheng et al. 2014)). Due to the incoherent DM-nucleon scattering inside the liquid core of neutron stars, the effective scattering cross section is uniquely determined by the absolute value of g_{np} (see Eq. (29)), thus the upper limit bounds with $g_{np} = -0.7$ are set between the bounds calculated with $g_{np} = 0$ and $g_{np} = 1$.

In addition, it is seen from Fig. 3 that the weakening or strengthening amplitudes for the bound on σ_p strongly depend on the nuclear interactions used. In particular, for the MSL1 interaction, which predicts a soft symmetry energy and an absence of protons in the neutron star core, the isospin-violating effects are much more significant than that in the Lc92 case with a stiffer symmetry energy and more protons inside the neutron star core.

In order to see more clearly the symmetry energy effects on the bound on σ_p , we show in Fig. 4 the exclusion contour of σ_p with MSL1 and Lc92 in the same panel for different values of g_{np} . Indeed, one can clearly see from Fig. 4 that the bound obtained from the MSL1 interaction with a soft symmetry energy is different apparently from that obtained from the Lc92 interaction with a stiffer symmetry energy. However, the specific values of these bounds vary with the isospin-violating factor g_{np} obviously. That is, on one hand, the MSL1 interaction predicts a neutron star with smaller radius but denser matter distribution relative to that predicted by

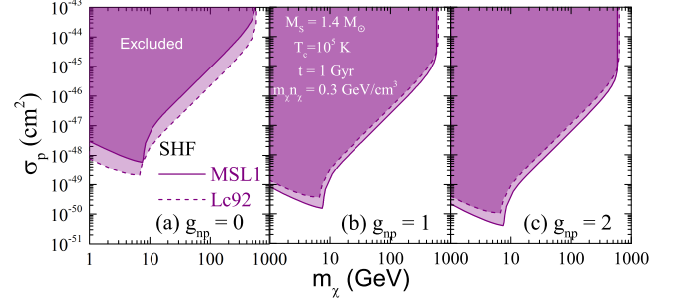


FIG. 4.— (Color online) Exclusion contour in m_χ - σ_p plane for the non-interacting bosonic asymmetric IVDM from a typical neutron star with $M_S = 1.4M_\odot$, $T_c = 10^5$ K, $t = 1$ Gyr and $m_\chi n_\chi = 0.3$ GeV/cm³ within SHF model with MSL1 and Lc92 for $g_{np} = 0$ (a), 1 (b) and 2 (c).

the Lc92 interaction (see the lower panel of Fig. 2). In this case, the factor f in Eq. (28) obtained from MSL1 will be larger than that in the Lc92 case, leading to a larger value of M_t as well as a smaller value of σ_p (panels (b) and (c) of Fig. 4). On the other hand, since the proton distribution predicted by each interaction is much different from each other, when the absolute value of g_{np} decreases (which means that the scattering process becomes more sensitive to the proton distribution inside the star), neutron stars with fewer protons (MSL1 case) become more transparent to the approaching DM particles, and thus the bound on σ_p weakens drastically in this case (panel (a) of Fig. 4).

Moreover, both the bending points and the cut-off mass lines obtained from these 2 interactions are also different from each other in Fig. 4. These variations further increase the differences among different bounds and lead to the overlap of various curves in Fig. 4.

3.3. The σ_p bounds from observation of realistic neutron stars

Based on the above discussions, in this subsection, we present the results of the constraint on σ_p for the non-interacting bosonic asymmetric IVDM from the observation of realistic old neutron stars. To avoid the complexity due to the evolution history of neutron stars in binary system, here we study an isolated old neutron star, i.e., PSR B1257+12 (Wolszczan 1990). The pulsar PSR B1257+12 is a planetary system with one solitary neutron star being orbited by three planets locating 0.6 kpc away from the solar system (Wolszczan & Frail 1992; Wolszczan 1994). When the neutron star's spin period and period derivative are accounted for, its age is determined to be 0.862 Gyr (Manchester et al. 2005).

For isolated neutron stars, their internal temperature is largely uncertain in observations, and usually one can use a simple analytical approximation to determine their internal temperature from the well studied surface temperature (T_s) (Gudmundsson et al. 1982), i.e.,

$$T_b = 1.288 \times 10^8 \text{ K} \left[\frac{10^{14} \text{ cm/s}^2}{g_s} \left(\frac{T_s}{10^6 \text{ K}} \right)^4 \right]^{0.455} \quad (56)$$

where $g_s = GM_S e^{-\phi(R_S)} / R_S^2$ is the surface gravity and T_b is the temperature at the bottom of the heat-blanketing envelope of the neutron star. Since the interior of a neutron star becomes isothermal within a few years af-

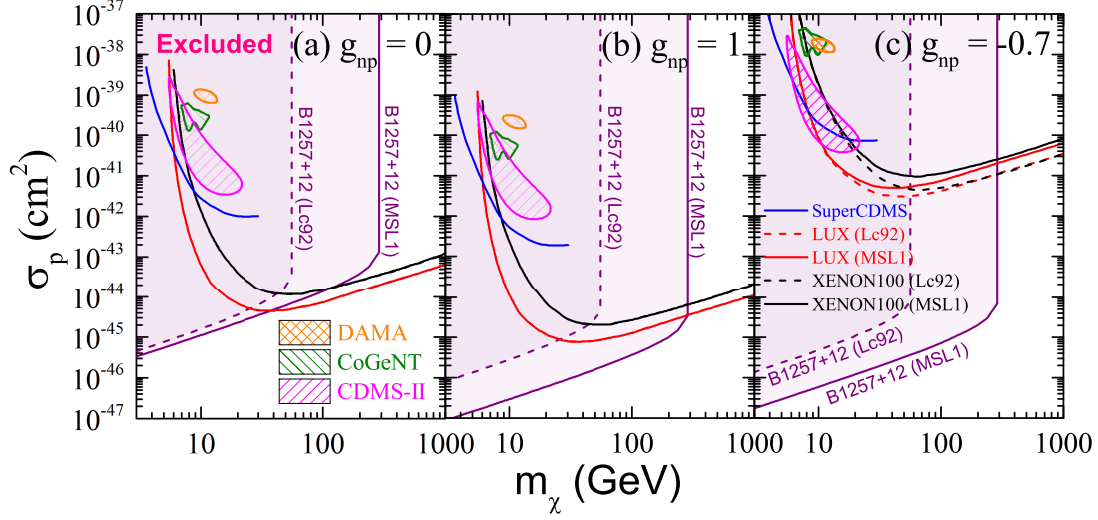


FIG. 5.— (Color online) Exclusion contour in m_χ - σ_p plane for the non-interacting bosonic asymmetric IVDM from PSR B1257+12 within SHF model with MSL1 and Lc92 for $g_{np} = 0$ (a), 1 (b) and -0.7 (c). The corresponding results from direct detection experiments, i.e., DAMA, CoGeNT, CDMS-II(Si), XENON100, LUX and SuperCDMS(Ge), are also included for comparison.

ter its birth (Page et al. 2004), we assume that the core temperature T_c of the neutron star equals to T_b in Eq. (56) in this work. Theoretically, the time evolution of the surface temperature of isolated neutron stars has been relatively well established and for solitary neutron stars older than several million years, their surface temperature is generally expected to be lower than 10^5 K (Yakovlev & Pethick 2004). In the present work, we assume a fixed value of $T_s = 10^5$ K for PSR B1257+12, and the σ_p bounds obtained from PSR B1257+12 with this assumption thus represent a conservative constraint since a lower T_s will lead to a stronger σ_p bound as will be shown later.

Adopting the standard neutron star mass of $1.4 M_\odot$ for PSR B1257+12 (Wolszczan & Frail 1992), we show in Fig. 5 the bounds for σ_p from the existence of the neutron star PSR B1257+12 within SHF model with MSL1 and Lc92 for $g_{np} = 0, 1$, and -0.7 , respectively. In the calculations, the halo parameters around the nearby neutron star PSR B1257+12 are assumed to have the same values as that around the earth, i.e., a Maxwell-Boltzmann distribution for $p(v)$ with $v_0 = 220$ km/s and a DM density of $m_\chi n_\chi = 0.3$ GeV/cm³. For comparison, we also show in Fig. 5 the corresponding results of the limits and regions from the direct detection experiments including the 90% confidence level (C.L.) limits from XENON100 (Aprile et al. 2012), LUX (Akerib et al. 2014) and SuperCDMS(Ge) (Agnese et al. 2014) along with the 90% C.L. favored regions from DAMA (Savage et al. 2009), CoGeNT (Aalseth et al. 2011) and CDMS-II(Si) (Agnese et al. 2013). The results of the direct detection experiments for various g_{np} are obtained according to the way introduced in Ref. (Zheng et al. 2014).

One can see from Fig. 5 that the bounds set by PSR B1257+12 are much stronger than that given by the direct detection experiments in the mass region about 10 GeV where a number of DM signals have been reported. Especially, it is interesting to see in Fig. 5 (c) that, for $g_{np} = -0.7$, which corresponds to the so-called xenophobic IVDM (Feng et al. 2013),

while the tension among various direct detection experiments is largely ameliorated due to the destructive interference of DM scattering with protons and neutrons inside the target nuclei (especially for Xenon target; see, e.g., (Zheng et al. 2014)), all the favored DM regions reported in direct detection experiments (i.e., DAMA, CoGeNT, and CDMS-II(Si)) are excluded by more than 3 orders of magnitude by the new limits obtained in the present work from the existence of PSR B1257+12.

In addition, comparing with the results shown in Fig. 4, one can see from Fig. 5 that the exclusion contours given by PSR B1257+12 become much weaker and the symmetry energy effects on the upper limits on σ_p as well as the cut-off mass lines become more pronounced. In particular, the values of the upper limits of σ_p are increased significantly and become comparable with (or even larger than) the limits given by LUX and XENON100 for massive IVDM in Fig. 5 (a) and (b). Such a weakening effect of the constraint on σ_p given by PSR B1257+12 is mainly due to the high surface temperature $T_s = 10^5$ K used for PSR B1257+12 which leads to a much higher core temperature $T_c = 1.95 \times 10^6$ K $\left(\frac{10^{14} \text{ cm}^3/\text{s}^2}{g_s}\right)^{0.455}$ (i.e., 1.4×10^6 K for MSL1 and 1.9×10^6 K for Lc92) than the fiducial value of 10^5 K used in Fig. 3 and Fig. 4. As a result, the value of N_{BEC} in Eq. (43) increases drastically, which dominates the inequality Eq. (46) and weakens the bounds on σ_p by more than two orders of magnitude.

4. CONCLUSIONS AND OUTLOOK

For non-interacting bosonic asymmetric dark matter (DM), the absence of the Fermi pressure and the ignorable dark matter self-annihilation could cause the formation of a DM boson star in the center of neutron stars through the interactions between DM particles and the neutron star matter, and the boson star could reach the Chandrasekhar limit to collapse into a black hole which may eventually destroy the host neutron star. The existence of old neutron stars therefore can provide important constraints on the interactions between the DM particles and nucleons. Since the nuclear matter inside

old neutron stars is generally highly isospin asymmetric (i.e., extremely neutron-rich), it is thus specially interesting to study the neutron star probe for isospin-violating dark matter (IVDM) which couples differently with protons and neutrons and provides a promising mechanism to ameliorate the tension among recent direct detection experiments.

In the present work, for the first time, by considering a realistic neutron star model in which the neutron star is assumed to be composed of β -stable and electrically neutral $npe\mu$ matter and its structure is obtained by solving the Tolman-Oppenheimer-Volkoff equations with equation of state of isospin asymmetric nuclear matter constrained by terrestrial experiments, we have investigated how the isospin violating DM-nucleon interactions and the symmetry energy in equation of state of isospin asymmetric nuclear matter influence the extraction of the bound on the DM-proton scattering cross-section σ_p from the existence of old neutron stars. In particular, we have restricted our attention on the non-interacting bosonic asymmetric IVDM within the mass region from 1 GeV to 1 TeV which is being extensively investigated by DM direct detection experiments. In addition, considering the large uncertainty on the density dependence of the symmetry energy, we have employed two EOSs with very different density dependences for the symmetry energy within the standard Skyrme-Hartree-Fock mean field model. Furthermore, all results given in this work, including the DM accretion by neutron stars and the BEC formation in the center of neutron stars, have been obtained self-consistently within the framework of general relativity.

Our results have indicated that, for a typical neutron star with mass $M_S = 1.4M_\odot$, center temperature $T_c = 10^5$ K, living age $t = 1$ Gyr and DM halo density $m_\chi n_\chi = 0.3 \text{ GeV/cm}^3$, the bounds on the σ_p can be varied by more than an order of magnitude depending on the specific values of the DM neutron-to-proton coupling

ratio f_n/f_p we adopted. Our results have also indicated that by considering the more realistic neutron star model rather than a simple uniform neutron sphere as usual, the symmetry energy effects which are presently largely unknown can also change the extraction of the bound on σ_p by more than a factor of 2.

Furthermore, we have studied how the observation of the realistic neutron star PSR B1257+12 constrains the σ_p . Our results have indicated that the observed nearby isolated old neutron star PSR B1257+12 can set a stringent limit for low-mass DM particles ($\leq 20 \text{ GeV}$) that reaches a sensitivity beyond the current best limits from direct detection experiments and excludes the DM interpretation of all previously-reported positive direct detection experimental results. Especially, our results have demonstrated that the existence of PSR B1257+12 excludes all the claimed DM regions reported in direct detection experiments (i.e., DAMA, CoGeNT, and CDMS-II(Si)) by more than 3 orders of magnitude for the specific IVDM with $g_{np} = -0.7$, namely, the so-called xenophobic IVDM, which has been proposed to ameliorate the tension among various direct detection experiments.

Our results in the present work are based on the assumption that IVDM is non-interacting bosonic asymmetric dark matter. It will be interesting to see how our results change if IVDM is self-interacting bosonic/fermionic asymmetric dark matter. These studies are in progress and will be reported elsewhere.

This work was supported in part by the Major State Basic Research Development Program (973 Program) in China under Contract No. 2015CB856904, the NNSF of China under Grant Nos. 11275125 and 11135011, the “Shu Guang” project supported by Shanghai Municipal Education Commission and Shanghai Education Development Foundation, the Program for Professor of Special Appointment (Eastern Scholar) at Shanghai Institutions of Higher Learning, and the Science and Technology Commission of Shanghai Municipality (11DZ2260700).

APPENDIX

DM THERMALIZATION AND BEC FORMATION IN NEUTRON STARS

It is important to take the general relativity corrections into account when we study the DM thermalization and BEC transition in neutron stars. Due to the strong gravitational field of the host neutron star, the space-time geometry in the neutron star core is warped so heavily that all results derived in Minkowski geometry should be in principle re-examined. Several attempts have been made recently (Jamison 2013), and we give a more precise derivation in this appendix.

The particle motion is governed by the geodesic equations. For DM particles with non-zero mass, by adopting the space-time geometry in Eq. (20), the geodesic equations can be expressed as (within the $\theta = \pi/2$ plane)

$$0 = \frac{d^2 r}{d\tau^2} + \frac{A'}{2A} \left(\frac{dr}{d\tau} \right)^2 - \frac{r}{A} \left(\frac{d\varphi}{d\tau} \right)^2 + \frac{B'}{2A} \left(\frac{dt}{d\tau} \right)^2 \quad (\text{A1})$$

$$0 = \frac{d^2 \varphi}{d\tau^2} + \frac{2}{r} \frac{d\varphi}{d\tau} \frac{dr}{d\tau} \quad (\text{A2})$$

$$0 = \frac{d^2 t}{d\tau^2} + \frac{B'}{B} \frac{dt}{d\tau} \frac{dr}{d\tau}, \quad (\text{A3})$$

where τ is the proper time and the prime denotes d/dr . The metric components A and B are given by Eqs. (34) and (35), respectively. Especially, since the energy density $\epsilon(r)$ and pressure $P(r)$ around the neutron star center are

approximately uniformly distributed, we treat them as constants (i.e., ϵ_c and P_c) in this work. Thus the gravitational mass $M(r)$ can be expressed as $M(r) = 4\pi r^3 \epsilon_c / 3$. Using the typical values of $\epsilon_c \sim 1 \text{ GeV}$ and $r \sim 1 \text{ m}$, we then have $2GM(r)/r \sim 10^{-8} \ll 1$ which means that the spatial part of the metric is almost Minkowski-like ($A(r) = 1$ according to Eq. (34)), and the geodesic equations can be further simplified as

$$0 = \frac{d^2 r}{d\tau^2} - r \left(\frac{d\varphi}{d\tau} \right)^2 + \frac{B'}{2} \left(\frac{dt}{d\tau} \right)^2 \quad (\text{A4})$$

$$0 = \frac{d^2 \varphi}{d\tau^2} + \frac{2}{r} \frac{d\varphi}{d\tau} \frac{dr}{d\tau} \quad (\text{A5})$$

$$0 = \frac{d^2 t}{d\tau^2} + \frac{B'}{B} \frac{dt}{d\tau} \frac{dr}{d\tau}. \quad (\text{A6})$$

Under the low speed approximation of $|d\mathbf{x}/d\tau| \ll 1$, where \mathbf{x} denotes the spatial part of the space-time coordinate of DM, Eqs. (A4) to (A6) can be rewritten as

$$\frac{d^2 \mathbf{x}}{dt^2} = -\nabla \Phi(r). \quad (\text{A7})$$

Here we have introduced an effective potential $\Phi(r)$ which is defined by

$$\Phi'(r) = B'(r)/2. \quad (\text{A8})$$

Substituting Eqs. (35) and (36) into the above equation, we then obtain

$$\begin{aligned} \Phi'(r) &= B(r)\phi'(r) \\ &\simeq \frac{4\pi}{3} Gr B_0 (\epsilon_c + 3P_c). \end{aligned} \quad (\text{A9})$$

The above equation is just the same as that of the Newton's gravitational potential except for replacing the mass density by $B_0(\epsilon_c + 3P_c)$. Here $B_0 = B(0)$ is the correction of the potential due to the non-trivial space-time curvature at the neutron star center (we note that B_0 has been simply set to be 1 in Ref. (Jamison 2013)). Therefore, the motion of a DM particle in the central region of the neutron star can be treated approximately as that it is moving in an external potential $\Phi(r)$. For thermalized DM following the Maxwell-Boltzmann distribution (Kouvaris & Tinyakov 2011; McDermott et al. 2012; Bramante et al. 2013)

$$p_{\text{th}}(v) = \sqrt{\frac{2}{\pi} \left(\frac{m_\chi}{T_c} \right)^3} v^2 \exp \left(\frac{-m_\chi v^2}{2T_c} \right), \quad (\text{A10})$$

the typical thermal radius r_{th} given in Eq. (42) can be obtained by assuming the average kinetic energy of the distribution equals to the potential energy, i.e.,

$$m_\chi \Phi(r_{\text{th}}) = \frac{1}{2} m_\chi v_{\text{rms}}^2, \quad (\text{A11})$$

where $v_{\text{rms}} = \sqrt{3T_c/m_\chi}$ is the root mean square speed of the distribution. The similar process can be applied to derive Eq. (44) for the BEC radius by assuming the zero point energy of the DM in the BEC phase confined in the potential $\Phi(r)$ equals to the potential energy.

Moreover, the BEC in an external potential has been well studied in Ref. (Bagnato et al. 1987). For a fixed temperature T_c , the critical number N_{BEC} of scalar particles with mass m in a harmonic oscillator potential $U(r) = \varepsilon(r/a)^2$ is given by

$$N_{\text{BEC}} = \zeta(3) T_c^3 \left(\frac{ma^2}{2\varepsilon} \right)^{\frac{3}{2}}. \quad (\text{A12})$$

Using the potential $\Phi(r)$ derived above, we then obtain the critical number in Eq. (43).

REFERENCES

- | | |
|--|---|
| <p>Aalseth, C. E., et al. 2011, Phys. Rev. Lett., 106, 131301
 Abrahamyan, S., et al. 2012, Phys. Rev. Lett., 108, 112502
 Ade, P. A. R., et al. 2013, arXiv:1303.5076
 Agnese, R., et al. 2013, Phys. Rev. D, 88, 031104
 Agnese, R., et al. 2013, Phys. Rev. Lett., 111, 251301
 Agnese, R., et al. 2014, arXiv:1402.7137
 Akerib, D. S., et al. 2014, Phys. Rev. Lett., 112, 091303
 Angloher, G., et al. 2012, European Physical Journal C, 72, 1971
 Aprile, E., et al. 2011, Phys. Rev. Lett., 107, 131302
 Aprile, E., et al. 2012, Phys. Rev. Lett., 109, 181301</p> | <p>Bagnato, V., Pritchard, D. E., & Kleppner, D. 1987, Phys. Rev. A, 35, 4354
 Baym, G., Pethick, C., & Sutherland, P. 1971, Astrophys. J., 170, 299
 Bell, N. F., Melatos, A., & Petraki, K. 2013, Phys. Rev. D, 87, 123507
 Bertoni, B., Nelson, A. E., & Reddy, S. 2013, arXiv:1309.1721
 Bertone, G., & Fairbairn, M. 2008, Phys. Rev. D, 77, 043515
 Bramante, J., Fukushima, K., & Kumar, J. 2013, Phys. Rev. D, 87, 055012</p> |
|--|---|

- Bramante, J., Fukushima, K., Kumar, J., & Stopnitzky, E. 2014, Phys. Rev. D, 89, 015010
- Carriere, J., Horowitz, C. J., & Piekarewicz, J. 2003, Astrophys. J., 593, 463
- Chabanat, E., Bonche, P., Haensel, P., Meyer, J., & Schaeffer, R. 1997, Nucl. Phys. A, 627, 710
- Chang, S., Liu, J., Pierce, A., Weiner, N., & Yavin, I. 2010, JCAP, 08, 018
- Chen, L. W. 2011, Sci. China: Phys. Mech. Astro., 54, (Suppl. 1) s124
- Chen, L. W. 2011, Phys. Rev. C, 83, 044308
- Chen, L.-W et al. 2001, Phys. Rev. C, 64, 064315
- Chen, L. W., & Gu, J. Z. 2012, J. Phys. G, 39, 035104
- Chen, L. W., Ko, C. M., Li, B. A., & Xu, J. 2010, Phys. Rev. C, 82, 024321
- Cirigliano, V., Graesser, M. L., Ovanesyan, G., & Shoemaker, I. M. 2013, arXiv:1311.5886
- Cline, J. M., & Frey, A. R. 2011, Phys. Rev. D, 84, 075003
- Colpi, M., Shapiro, S. L., & Wasserman, I. 1986, Phys. Rev. Lett., 57, 2485
- de Lavallaz, A., & Fairbairn, M. 2010, Phys. Rev. D, 81, 123521
- Feng, J. L., Kumar, J., Marfatia, D., Sanford, D. 2011, Phys. Lett. B, 703, 124-127
- Feng, J. L., Kumar, J., & Sanford, D. 2013, Phys. Rev. D, 88, 015021
- Feng, J. L., Kumar, J., Marfatia, D., & Sanford, D. 2013, arXiv:1307.1758.
- Fitzpatrick, A. L., & Zurek, K. M. 2010, Phys. Rev. D, 82, 075004
- Frandsen, M. T., Kahlhoefer, F., Sarkar, S., & Schmidt-Hoberg, K. 2011, JHEP, 1109, 128
- Friedrich, J., & Reinhard, P.-G. 1986, Phys. Rev. C, 33, 335
- Gao, X., Kang, Z., & Li, T. 2013, JCAP, 01, 021
- Giuliani, F. 2005, Phys. Rev. Lett., 95, 101301
- Goldman, I., & Nussinov, S. 1989, Phys. Rev. D, 40, 3221
- Gonzalez, D., & Reisenegger, A. 2010, A&A, 522, A16
- Gould, A. 1987, Astrophys. J., 321, 571
- Gudmundsson, E. H., Pethick, C. J., & Epstein, R. I. 1982, Astrophys. J., 259, L19
- Guver, T., Erkoca, A. E., Reno, M. H., & Sarcevic, I. 2014, JCAP, 05, 013
- He, X.-G., Ren, B., & Tandeau, J. 2012, Phys. Rev. D, 85, 093019
- Ho, C. M., & Scherrer, R. J. 2013, Phys. Lett. B, 722, 341
- Horowitz, C. J. 2012, arXiv:1205.3541
- Iida, K., & Sato, K. 1997, Astrophys. J., 477, 294
- Jamison, A. O. 2013, Phys. Rev. D, 88, 035004
- Klüpfel, P., Reinhard, P.-G., Bürvenich, T.J., & Maruhn, J. A. 2009, Phys. Rev. C, 79, 034310
- Kouvaris, C. 2008, Phys. Rev. D, 77, 023006
- Kouvaris, C. 2012, Phys. Rev. Lett., 108, 191301
- Kouvaris, C. 2013, Adv. High Energy Phys., Vol. 2013, Article ID 856196
- Kouvaris, C., & Tinyakov, P. 2011, Phys. Rev. Lett., 107, 091301
- Kurylov, A., & Kamionkowski, M. 2004, Phys. Rev. D, 69, 063503
- Lattimer, J. M., & Prakash, M. 2000, Phys. Rep., 333, 121.
- Lattimer, J. M., & Prakash, M. 2001, Astrophys. J., 550, 426
- Lattimer, J. M., & Prakash, M. 2004, Science, 304, 536
- Li, B. A., Chen, L. W., & Ko, C. M. 2008, Phys. Rep., 464, 113
- Link, B., Epstein, R. I., & Lattimer, J. M. 1999, Phys. Rev. Lett., 83, 3362
- Manchester, R. N., Hobbs, G. B., Teoh, A., & Hobbs, M. 2005, Astron. J. 129, 1993,
<http://www.atnf.csiro.au/people/pulsar/psrcat/>
- McDermott, S. D., Yu, H.-B., & Zurek, K. M. 2012, Phys. Rev. D, 85, 023519
- Nagao, K. I., & Naka, T. 2013, Prog. Theor. Exp. Phys. B, 02, 043
- Nobile, E. D., Kouvaris, C., Sannino, F., & Virkajarvi, J. 2012, Mod. Phys. Lett. A, 27, 1250108
- Okada, N., & Seto, O. 2013, Phys. Rev. D, 88, 063506
- Page, D., Lattimer, J. M., Prakash, M., & Steiner, A. W. 2004, ApJS, 155, 623
- Petraki, K. & Volkas, R. R. 2013, Int. J. Mod. Phys. A, 28, 1330028
- Press, W.H., & Spergel, D.N. 1985, Astrophys. J., 296, 679
- Savage, C., et al. 2009, JCAP, 0904, 010
- Shapiro, S. L., & Teukolsky, S. A. 1983, Wiley, New York, 1983, p. 569
- Smith, M. C., et al. 2007, Mon. Not. R. Astron. Soc., 379, 755
- Wolszczan, A. 1990, IAU Circ., 5073, 1
- Wolszczan, A., & Frail, D. A. 1992, Nature, 355, 145
- Wolszczan, A. 1994, Science, 264, 538
- Xu, J., Chen, L. W., Li, B. A., & Ma, H. R. 2009, Astrophys. J., 697, 1549
- Yakovlev, D. G., & Pethick, C. J. 2004, ARA&A, 42, 169
- Zhang, Z., & Chen, L. W. 2013, Phys. Lett. B, 726, 234
- Zheng, H., & Chen, L. W. 2012, Phys. Rev. D, 85, 043013
- Zheng, H., Zhang, Z., & Chen, L. W. 2014, JCAP, 08, 011
- Zurek, K. M. 2014, Phys. Rep., 537, 91